

# Thermophysical properties of the lanthanide sesquisulfides.

## III. Determination of Schottky and lattice heat-capacity contributions of $\gamma$ -phase $\text{Sm}_2\text{S}_3$ and evaluation of the thermophysical properties of the $\gamma$ -phase $\text{Ln}_2\text{S}_3$ subset

Roey Shaviv<sup>a)</sup> and Edgar F. Westrum, Jr.

*Department of Chemistry, University of Michigan, Ann Arbor, Michigan 48109-1055*

John. B. Gruber

*Department of Physics, San Jose State University, San Jose, California 95192-0106*

B. J. Beaudry and P. E. Palmer

*Ames Laboratory, Iowa State University, Ames, Iowa 50011-3020*

(Received 18 October 1991; accepted 10 January 1992)

We report the experimental heat capacity of  $\gamma$ -phase  $\text{Sm}_2\text{S}_3$  and derived thermophysical properties at selected temperatures. The entropy, enthalpy increments, and Gibbs energy function are  $21.50R$ ,  $3063R \cdot \text{K}$ , and  $11.23R$  at 298.15 K. The experimental heat capacity is made up of lattice and electronic (Schottky) contributions. The lattice contribution is determined for all  $\gamma$ -phase lanthanide sesquisulfides ( $\text{Ln}_2\text{S}_3$ ) using the Komada/Westrum model. The difference between the experimental heat capacity and the deduced lattice heat capacity is analyzed as the Schottky contribution. Comparisons are made between the calorimetric Schottky contributions and those determined based on crystal-field electronic energy levels of  $\text{Ln}^{3+}$  ions in the lattice and between the Schottky contributions obtained from the empirical volumetric priority approach and from the Komada/Westrum theoretical approach. Predictions for the thermophysical properties of  $\gamma$ -phase  $\text{Eu}_2\text{S}_3$  and  $\gamma$ -phase  $\text{Pm}_2\text{S}_3$  (unavailable for experimental determination) are also presented.

### INTRODUCTION

The first two papers in this series<sup>1,2</sup> describe the experimental determination and the resolution of the heat capacities of  $\text{La}_2\text{S}_3$ ,<sup>1</sup>  $\text{Ce}_2\text{S}_3$ ,<sup>1</sup>  $\text{Nd}_2\text{S}_3$ ,<sup>1</sup>  $\text{Gd}_2\text{S}_3$ ,<sup>1</sup>  $\text{Pr}_2\text{S}_3$ ,<sup>2</sup>  $\text{Tb}_2\text{S}_3$ ,<sup>2</sup> and  $\text{Dy}_2\text{S}_3$  (Ref. 2) all of which are isostructural,  $\gamma$ -phase members of the lanthanide sesquisulfide system. Most of these lanthanide ( $\text{Ln}_2\text{S}_3$ ) compounds exhibit—in addition to their lattice heat-capacity contribution—excess contributions as a result of the electrons in the  $4f^n$  shell of the lanthanide ion.<sup>3-6</sup> The study of these phenomena by calorimetric, spectroscopic, and magnetic techniques—as previously noted<sup>1,2</sup>—has led to the resolution of their energetic spectra. The electronic configuration of the  $4f$  orbitals and the crystal-field splitting of these orbitals, which causes the removal of some degeneracies, gives rise to Schottky contributions to the heat capacities. Analysis of the crystal-field splittings, the infrared and Raman spectra, and the magnetic susceptibilities of these compounds are consistent with the resolution of the observed heat capacities.

Cryogenic heat-capacity measurements provide an important technique for the study of the Schottky and magnetic contributions of these materials. Resolving these excess contributions from the typically larger lattice contribution

by the volumetric scheme<sup>7</sup> for estimation of lattice heat capacity was found to be useful—as it was for the bixbyite sesquioxides.<sup>8</sup>

The main task in the analysis of the heat-capacity values in this system is the resolution of the electronic heat capacity. As illustrated in the previous papers in this series<sup>1,2</sup> in solid lanthanide compounds the electronic heat capacity takes the form of a Schottky contribution which is the heat capacity of a system with a finite number of energy levels. The lowest level is defined as the zero energy of the system. Each level  $i$  has a degeneracy  $g_i$  and an energy  $E_i$  above the ground level. The heat capacity of this system is

$$C_v(T, E, g) = \frac{g_1 R}{(qkT)^2} \left[ \sum_{i=2}^n g_i E_i^2 e^{-E_i/kT} + \sum_{i=2}^{n-1} \sum_{j=i+1}^n \frac{g_i g_j}{g_1} (E_j - E_i)^2 e^{-E_i + E_j/kT} \right],$$

which is equivalent to

$$C_v(T, E, g) = \frac{g_1 R}{(kT)^2} \left[ \frac{1}{q} \sum_{i=1}^n g_i E_i^2 e^{-E_i/kT} - \frac{1}{q^2} \left( \sum_{i=1}^n g_i E_i e^{-E_i/kT} \right)^2 \right],$$

where  $R$  is the universal gas constant,  $E_i$  and  $g_i$  are the energy and degeneracy of the  $i$ th state, respectively, and  $q$  is the partition function for the system.  $T$  is the temperature and  $k$  is the Boltzmann constant. For a system in which  $n \rightarrow \infty$ ,  $E_i = iE_2$ , and  $g_i = g_1$  for all  $i$  values, the Schottky heat-

<sup>a)</sup> Current address: Department of Chemistry, University of Illinois at Chicago, Chicago, Illinois 60680.

capacity function reduces rigorously to an Einstein heat-capacity function.

For the special case in which a large energy gap exists between a subset of lower energy levels and any higher energy level the heat capacity, due to thermal excitation in the lower levels, will be unaffected by the higher levels and exhibit Schottky-type morphology. The lanthanide compounds are an example of such a system. In the  $\text{Ln}_2\text{S}_3$  system the typical energy spacing in the lower set of electronic energy levels is about 100 to 400  $\text{cm}^{-1}$ . The origin of this low-energy spacing is the removal of the degeneracy of  $4f$  orbitals by the crystalline electric field.

The Schottky contributions observed in this system are broad and may cover the entire experimental temperature range. Phenomena of such breadth pose a difficulty in their resolution because there is but little direct experimental information about the lattice contributions. Excess contributions can often be analyzed by graphical means since the lattice contribution, outside the affected temperature range, is known. When broad contributions are present, the lattice heat capacity must be evaluated independently—as is necessary in the analysis of the heat-capacity data in the present system. The volume-weighted lattice approximation has been used previously with success for several other groups of lanthanide compounds,<sup>7-14</sup> as well as for some of the sesquisulfides. Its application to the lanthanide sesquisulfides was presented in the first two papers of this series.<sup>1,2</sup> The use of the volume-weighted lattice-approximation technique is, however, presumed to be most appropriate where the relevant compounds are isostructural or is one where the ions have at least the same coordination numbers.

The Komada/Westrum phonon distribution model<sup>15-18</sup> provides the means to overcome the limitations of the volumetric method. The model calculates a lattice heat capacity based upon structural and physical properties. Moreover, similarities between compounds may be utilized to interpolate between reference compounds. Thus the method allows—by means of three related computer programs called “LEM” programs—evaluation of the lattice contribution of compounds in an isostructural series based upon known lattice heat capacities of related-isostructural compounds.

This paper also reports on the measurements and interpretation of the thermophysical properties of yet another—the last accessible—member of the  $\gamma$ -phase lanthanide sesquisulfide subset,  $\text{Sm}_2\text{S}_3$ . Two other members of this subset—not available for measurement—are  $\text{Pm}_2\text{S}_3$  and  $\text{Eu}_2\text{S}_3$ . The former is not readily available because of the nuclear instability of promethium, the latter by reasons of the relative instability of the III oxidation state of europium. Their thermophysical properties have been evaluated by applying the Komada/Westrum approximation for the lattice heat capacity and by using lattice-sum calculations to estimate the crystalline electric field splittings.

## EXPERIMENT

### Sample provenance and characterization

The samarium sesquisulfide sample was prepared at the Ames Laboratory by direct combination of the pure ele-

ments in a manner similar to that described earlier.<sup>1</sup> The samarium metal used was prepared in the Ames Laboratory and has the chemical analysis typical of the highly purified materials produced in that laboratory.<sup>19</sup> Sublimed sulfur (99.999%) was obtained from ASARCO.<sup>20</sup>

In the preparation of  $\text{Sm}_2\text{S}_3$ , stoichiometric quantities of samarium and sulfur were sealed in a quartz ampoule. The sealed ampoule was then heated slowly to 575 °C, and held for two weeks at this temperature by which time all sulfur had reacted. The ampoule was then heated slowly to 1000 °C, held there for three days, cooled to room temperature, and opened. The sulfide was ground and sieved to 200 mesh powder. The powder was cold pressed into pellets 4 mm thick by 15 mm diameter. The pressed pellets were heated to 1350 °C under a dynamic  $\text{H}_2\text{S}$  atmosphere for 9 h. A small random portion was removed for x-ray and chemical analysis.

Debye-Scherrer x-ray patterns contained only lines of the  $\gamma$ -phase structure. The lattice parameter  $a_0$  is determined in this study to be  $(8.4383 \pm 0.0001)$  Å while the literature value<sup>21</sup> is 8.448 Å. The final S to Sm ratio determined by chemical analysis is  $1.499 \pm 0.003$ .

### Automated adiabatic calorimetry

The data were taken in the Mark X calorimetric cryostat, an improved version<sup>22</sup> of the Mark II cryostat previously described.<sup>23</sup> Data acquisition was computer assisted. Information on the initial, final, and mean temperatures, on the energy input and the resistance of the heater, together with the apparent heat capacity of the system were recorded. A gold-plated, oxygen-free, high-conductivity (OFHC) copper calorimeter (laboratory designation W-61) was employed in the measurement. The calorimeter is especially equipped with two pairs of perforated copper, spring-loaded sleeves, soldered to the heater-thermometer well, to hold the sample pellets. After loading, and soldering the cover in place (with Cerroseal solder—50 mass % of Sn and In) the calorimeter was evacuated and approximately 2 kPa (at about 300 K) helium gas were added to facilitate rapid thermal equilibration. The temperatures were measured with a Leeds & Northrup platinum-encapsulated, platinum-resistance thermometer which was calibrated by the National Bureau of Standards against the IPTS-48 temperature scale. All other quantities were referenced to standards of the National Bureau of Standards.

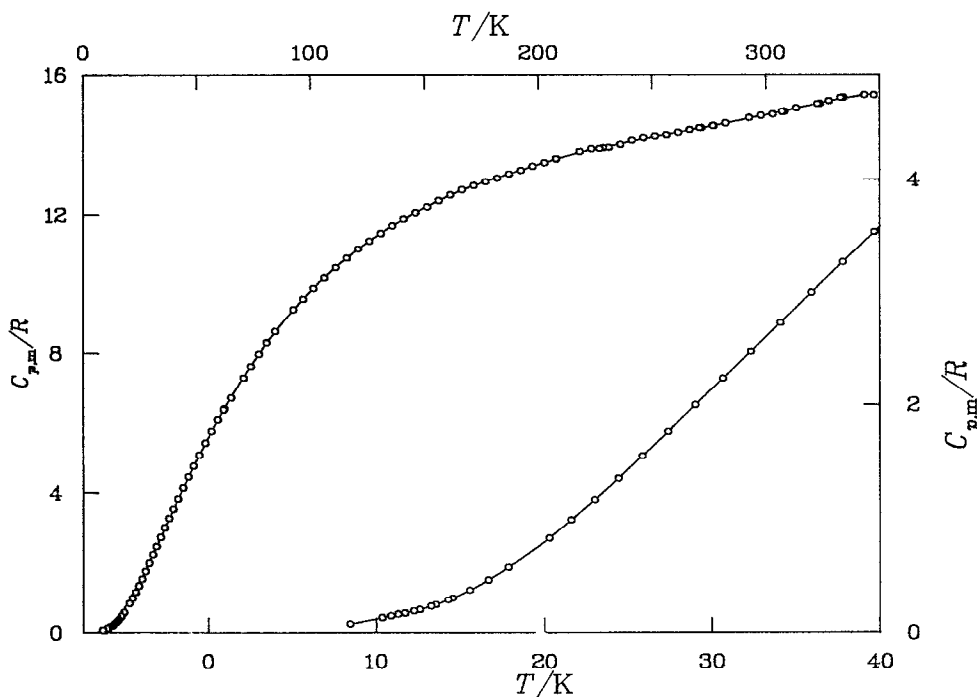
### Optical spectroscopy

Samarium sesquisulfide used for the optical spectra experiments was prepared in powder form by the method introduced by Henderson *et al.*<sup>24</sup> Chemical analysis indicated the product was  $\text{SmS}_{1.500 \pm 0.003}$ . X-ray powder patterns showed that the material had the  $\text{Th}_3\text{P}_4$  defect structure representing the high temperature  $\gamma$  phase. Single crystals of  $\text{Sm}_2\text{S}_3$  could not be grown even under conditions of different temperatures and various pressures of sulfur vapor. The melted ingots obtained after heating the powder in pyrolytic graphite crucibles were black and contained many very small crystallites.<sup>25</sup> Chemical analyses of the ingots revealed

TABLE I. Molar heat capacities of samarium sesquisulfide.\*

$(R = 8.3144 \text{ J K}^{-1} \text{ mol}^{-1})$									
$T(\text{K})$	$C_{p,m}/R$	$T(\text{K})$	$C_{p,m}/R$	$T(\text{K})$	$C_{p,m}/R$	$T(\text{K})$	$C_{p,m}/R$	$T(\text{K})$	$C_{p,m}/R$
Samarium sesquisulfide, $\text{Sm}_2\text{S}_3$ , $M = 396.98 \text{ g mol}^{-1}$									
Series I									
		285.971	6.783*	115.839	10.746	11.301	0.161	44.035	4.145
		290.672	27.219*	120.801	11.011	12.246	0.189	44.035	4.145
302.146	14.947*	294.693	27.715*	125.781	11.241	13.267	0.231	46.316	4.454
307.067	14.934	300.991	13.810*	130.766	11.463	14.285	0.288	46.316	4.454
312.246	15.191*	306.459	29.370*	135.755	11.682			48.609	4.759
317.461	14.732*	310.825	29.893*	140.759	11.877	Series VI		48.609	4.759
322.657	15.159			130.748	11.459			51.106	5.079
327.710	15.251	Series III		135.796	11.683	9.694	0.135*	51.106	5.079
332.899	15.346			140.905	11.882	10.874	0.146	53.796	5.423
338.089	15.295*	64.580	6.808*	146.017	12.057	11.711	0.171	53.796	5.423
343.279	15.425	66.626	6.934*	151.140	12.221	12.591	0.201	56.494	5.755
347.672	15.644*	69.729	7.253*	156.267	12.395	13.547	0.245	56.494	5.755
		72.700	7.518*	161.395	12.549	14.561	0.305	59.211	6.083
Series II		75.928	7.854*	166.528	12.699	15.573	0.377	59.211	6.083
		79.402	8.190*	171.684	12.818	16.682	0.467	62.088	6.397
226.825	13.888			176.837	12.932	17.878	0.577	65.124	6.708
231.047	13.920	Series IV		181.990	13.036	19.089	0.692*		
236.124	14.003			187.145	13.162	20.302	0.834	Series VII	
241.185	14.125	61.790	6.362	192.302	13.267	21.610	0.991		
246.252	14.196	64.698	6.725*	197.459	13.384	23.012	1.168	270.893	14.478
251.336	14.239	67.641	7.029*	202.629	13.488	24.424	1.355	277.105	14.534
256.419	14.274	70.609	7.282	207.797	13.595	25.857	1.552	282.286	14.611
261.493	14.345	73.820	7.618	212.976	13.630*	27.389	1.765	287.471	14.583
266.573	14.424	77.282	7.970	218.146	13.799	29.015	1.998	292.647	14.763
271.652	14.477	80.752	8.303	223.320	13.878	30.655	2.235	297.817	14.826
276.734	14.535	84.479	8.634	228.496	13.905	32.311	2.475	303.004	14.864
281.805	14.676*	88.454	9.009*			34.071	2.732	308.191	14.943
287.398	9.093*	92.452	9.272	Series V		35.929	3.002	313.369	15.041
292.001	26.906*	96.713	9.576			37.799	3.269	318.537	15.229
296.070	27.535*	101.229	9.876	8.436	0.075	39.683	3.538	323.746	15.172
302.219	13.676*	105.953	10.175	9.329	0.125*	41.765	3.829	328.926	15.429
307.573	29.153*	110.895	10.472	10.351	0.130	41.765	3.829	334.108	15.356

\*\*Not included in the calculation of thermodynamic properties.

FIG. 1. Experimental subambient heat capacity of  $\text{Sm}_2\text{S}_3$ . Lower temperature data are presented in the lower right corner on an expanded scale.

that some of the samarium had been reduced to the divalent state.

To obtain absorption spectra of  $\text{Sm}_2\text{S}_3$ , mulls were prepared by mixing some of the original powder with an inert transparent gel.<sup>26</sup> The mixture was placed between two quartz slides and inserted into a conduction dewar having a copper block with a vertical slit just large enough to hold the sample. A matrix was added to improve thermal conductivity between the sample and block. A temperature sensor was included in the mull between the quartz plates which gave readings of 20 and 90 K when the Dewar was filled with liquid helium and liquid nitrogen, respectively. Spectra were obtained between 2.5 and 0.30  $\mu\text{m}$  using a Cary Model 14R.

## RESULTS AND DISCUSSION

### Samarium sesquisulfide

#### Heat capacity

The experimental heat-capacity data for  $\text{Sm}_2\text{S}_3$  are presented in Table I and plotted in Fig. 1. Thermodynamic functions at selected temperatures are presented in Table II. The behavior of the heat-capacity curve at temperatures that are lower than the experimental lowest temperatures were predicted using the LEM-2 program.<sup>15</sup> Excess heat-capacity contributions (such as the Schottky contribution which is significant at higher temperatures) are negligible below 8 K, and consequently were not taken into account for the calculation of the thermodynamic functions below that temperature. The experimental standard deviations in these measurements decrease gradually from about  $\pm 4\%$  at 7 K to about  $\pm 0.1\%$  at 20 K and remain below that value at higher temperatures.

The lattice heat capacity for  $\text{Sm}_2\text{S}_3$  was found by employing the Komada/Westrum approximation to lattice heat capacity.<sup>15-18</sup> The Schottky contribution from the electronic energy-level splitting was thus deduced from the observed total heat capacity of the compound by subtracting the calculated lattice contribution.

#### Analysis of hot bands in the absorption spectra

$\text{Sm}_2\text{S}_3$  forms a body-centered cubic ( $\text{Th}_3\text{P}_4$ -phase) lattice which is usually referred to as the  $\gamma$  phase. The symmetry group is  $I\bar{4}3d$  and contains 16/3 formula units in a unit cell. Vacancies exist in the metal sites and have a disordered arrangement. The cations are in the unusual octocoordinated environment<sup>27</sup> of a triangular dodecahedron, which can be regarded as formed by the superposition of two tetrahedra, one of which is flat and the other elongated. The point-group symmetry of the cation is  $S_4$ . This structure is found in all light lanthanide sesquisulfide compounds.

The  $^{2S+1}L_J$  ground state of  $\text{Sm}^{3+}$  ( $4f^5$ ) is  $^6H_{5/2}$ . The crystal field of the lattice splits the state into three electronic energy levels. Each level is doubly degenerate. The first excited  $^{2S+1}L_J$  state ( $^6H_{7/2}$ ) is found near 1100  $\text{cm}^{-1}$ . This state is split by the crystal field into four doubly degenerate electronic levels. Higher states such as  $^6H_{9/2}$ ,  $^6H_{11/2}$ , etc., are so much higher in energy that their contribution to the sub-ambient heat capacity is negligible.

The crystal-field splitting of the ground state manifold,

$^6H_{5/2}$ , can be obtained by analyzing the temperature dependent (hot band) spectra.<sup>28</sup> Hot bands represent electronic transitions from the two excited electronic levels of  $^6H_{5/2}$  to electronic levels in the various excited  $^{2S+1}L_J$  manifolds of  $\text{Sm}^{3+}$ . Isolated excited manifolds such as  $^4G_{5/2}$  (565 nm) and  $^4F_{3/2}$  (532 nm) were especially useful in obtaining hot band data which indicate the splitting of  $^6H_{5/2}$  is 0, 84, and 194  $\text{cm}^{-1}$ .<sup>28</sup>

A crystal-field splitting analysis of some 46 excited crystal-field electronic energy levels of  $\text{Sm}^{3+}$  in manifolds including  $^6F_J$  and  $^6H_J$  multiplets yields an rms deviation of 10  $\text{cm}^{-1}$  between calculated and experimental levels.<sup>29</sup> Using the set of  $B_{km}$  parameters from that calculation,  $B_{20} = 365 \text{ cm}^{-1}$ ,  $B_{40} = -620 \text{ cm}^{-1}$ ,  $B_{44} = 765 \text{ cm}^{-1}$ ,  $B_{60} = -22 \text{ cm}^{-1}$ ,  $B_{64}(R) = 620 \text{ cm}^{-1}$ , and  $B_{64}(I) = 0 \text{ cm}^{-1}$ , we predict a splitting for the  $^6H_{7/2}$  manifold which is useful for the purpose of determining the Schottky contribution to the heat capacity of  $\text{Sm}_2\text{S}_3$ .<sup>30</sup> The predicted splitting is 1085, 1106, 1205, and 1214  $\text{cm}^{-1}$ . The observed electronic energy levels of  $^6H_{5/2}$  and the calculated levels for  $^6H_{7/2}$  are given in Table III. These energy levels are used to predict the spectroscopic Schottky contributions appearing in Fig. 5.

#### Resolution of the heat capacities of $\gamma$ -phase sesquisulfides

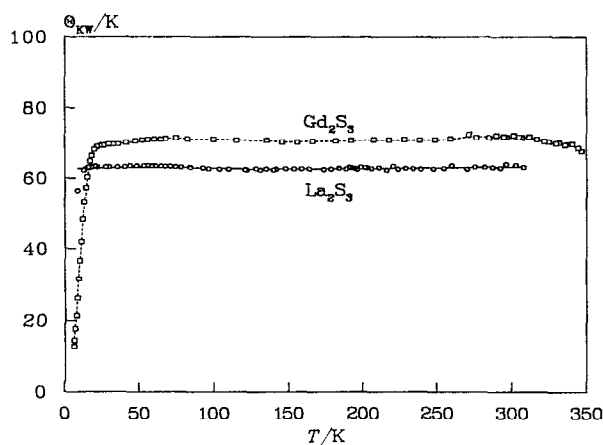
The experimental heat capacities of the  $\gamma$ -phase lanthanide sesquisulfides were resolved with the Komada/Westrum phonon distribution model.<sup>15-18</sup> Characteristic temperatures,  $\Theta_{\text{KW}}$ 's, were calculated on the basis of the experimental heat capacities of  $\text{La}_2\text{S}_3$  and  $\text{Gd}_2\text{S}_3$  in which excess heat capacity is not present (with the exception of a resolvable magnetic ordering in  $\text{Gd}_2\text{S}_3$  at low temperatures). The Komada/Westrum model uses the temperature, the lattice heat capacity, and the molecular formula as primary input parameters. Other physical parameters, related to the masses and to the volumes of the atoms and to the size and number of atoms in a primitive cell, are also used as input coefficients to the LEM programs.<sup>15</sup> Alternatively, these additional coefficients may be supplied by default. The programs use these parameters and the lattice heat capacity to obtain a phonon distribution function which is represented by the single output parameter— $\Theta_{\text{KW}}$ —the apparent characteristic temperature. The constancy of  $\Theta_{\text{KW}}$  with temperature—in marked contrast to that of the corresponding Debye characteristic temperature—indicates that the lattice heat capacity is reproduced by the same phonon density of states function over an extended temperature region. Although the approximated phonon density of states may not be unique it provides a good predictor of the lattice heat capacity beyond the experimental range or between related compounds. Constancy of the characteristic temperatures may be enhanced by slightly modifying the input coefficients to better fit the experimental data.<sup>30</sup> Small adjustments of the coefficients were, therefore, used in evaluating the characteristic temperatures for  $\text{La}_2\text{S}_3$  and  $\text{Gd}_2\text{S}_3$ , resulting in apparent  $\Theta_{\text{KW}}$ 's which are nearly constant over the entire temperature region. Default coefficients, supplied by the program, were used when the actual physical parameters were not known. The resultant  $\Theta_{\text{KW}}$ 's for these two refer-

TABLE II. Thermodynamic properties at selected temperatures for samarium, promethium, and europium sesquisulfides (values for the latter two compounds are based on the theoretical prediction to their heat capacities).

$(R = 8.3144 \text{ J K}^{-1} \text{ mol}^{-1})$					$(R = 8.3144 \text{ J K}^{-1} \text{ mol}^{-1})$				
$T \text{ (K)}$	$C_{p,m}^0/R$	$\Delta_0^{\ddagger}S_m^0/R$	$\Delta_0^{\ddagger}H_m^0/R \cdot K$	$\Phi_m^0(T,0)/R$	$T \text{ (K)}$	$C_{p,m}^0/R$	$\Delta_0^{\ddagger}S_m^0/R$	$\Delta_0^{\ddagger}H_m^0/R \cdot K$	$\Phi_m^0(T,0)/R$
Samarium sesquisulfide, $\text{Sm}_2\text{S}_3$					Promethium sesquisulfide, $\text{Pm}_2\text{S}_3$				
0	0.0	0.0	0.0	0.0	160	13.453	14.589	1310.5	6.398
10	0.118	0.028	0.229	0.005	170	13.625	15.41	1445.9	6.905
15	0.335	0.110	1.274	0.025	180	13.777	16.19	1583.0	7.399
20	0.800	0.264	4.010	0.064	190	13.912	16.94	1721.4	7.882
25	1.435	0.509	9.552	0.127	200	14.033	17.66	1861.2	8.353
30	2.139	0.832	18.468	0.217	210	14.141	18.35	2002.0	8.812
35	2.867	1.217	30.980	0.331	220	14.239	19.01	2144.0	9.261
40	3.583	1.646	47.115	0.469	230	14.328	19.64	2286.8	9.698
45	4.275	2.109	66.77	0.625	240	14.409	20.25	2430.5	10.126
50	4.943	2.594	89.82	0.797	250	14.483	20.84	2575.0	10.542
60	6.157	3.605	145.47	1.180	260	14.551	21.41	2720.1	10.950
70	7.239	4.637	212.53	1.600	270	14.612	21.96	2866.0	11.347
80	8.219	5.668	289.91	2.044	280	14.669	22.49	3012.4	11.736
90	9.078	6.687	376.51	2.504	290	14.721	23.01	3159.3	12.116
100	9.807	7.683	471.04	2.972	298.15	14.761	23.42	3279.5	12.419
110	10.424	8.647	572.3	3.445	300	14.769	23.51	3306.8	12.487
120	10.958	9.577	679.2	3.917	325	14.874	24.70	3677.4	13.382
130	11.430	10.474	791.2	4.387	350	14.961	25.80	4050.3	14.230
140	11.845	11.336	907.6	4.853					
150	12.203	12.166	1027.9	5.313					
160	12.507	12.963	1151.5	5.766					
170	12.769	13.730	1277.9	6.212					
180	13.004	14.466	1406.8	6.651					
190	13.224	15.18	1538.0	7.081					
200	13.434	15.86	1671.3	7.503					
210	13.628	16.52	1806.6	7.916					
220	13.801	17.16	1943.8	8.322					
230	13.950	17.77	2082.5	8.720					
240	14.081	18.37	2222.7	9.109					
250	14.205	18.95	2364.1	9.492					
260	14.330	19.51	2506.8	9.866					
270	14.461	20.05	2650.8	10.233					
280	14.590	20.58	2796.0	10.593					
290	14.714	21.09	2942.6	10.947					
298.15	14.813	21.50	3062.9	11.230					
300	14.836	21.59	3090.3	11.293					
325	15.22	22.80	3465.7	12.132					
350	15.43	23.93	3849.8	12.935					
Promethium sesquisulfide, $\text{Pm}_2\text{S}_3$					Europium sesquisulfide, $\text{Eu}_2\text{S}_3$				
0	0.0	0.0	0.0	0.0	0	0.0	0.0	0.0	0.0
10	0.048	0.013	0.101	0.003	10	0.074	0.021	0.162	0.005
15	0.234	0.061	0.723	0.013	15	0.279	0.085	0.985	0.019
20	0.635	0.178	2.801	0.038	20	0.617	0.209	3.177	0.050
25	1.246	0.382	7.424	0.085	25	1.053	0.392	7.319	0.099
30	2.016	0.675	15.526	0.157	30	1.556	0.627	13.818	0.167
35	2.890	1.050	27.759	0.257	35	2.103	0.908	22.950	0.252
40	3.822	1.497	44.524	0.384	40	2.682	1.226	34.903	0.354
45	4.769	2.002	66.00	0.535	45	3.284	1.577	49.812	0.470
50	5.701	2.553	92.19	0.709	50	3.904	1.955	67.78	0.599
60	7.420	3.748	158.00	1.114	60	5.175	2.778	113.15	0.893
70	8.854	5.003	239.62	1.580	70	6.458	3.673	171.32	1.225
80	9.985	6.262	334.06	2.087	80	7.709	4.617	242.20	1.590
90	10.852	7.491	438.44	2.619	90	8.887	5.594	325.25	1.980
100	11.514	8.670	550.4	3.166	100	9.962	6.587	419.59	2.391
110	12.025	9.792	668.2	3.718	110	10.916	7.582	524.1	2.818
120	12.429	10.857	790.6	4.269	120	11.744	8.568	637.5	3.256
130	12.756	11.865	916.6	4.814	130	12.452	9.537	758.6	3.702
140	13.027	12.820	1045.5	5.353	140	13.050	10.482	886.2	4.153
150	13.256	13.727	1177.0	5.881	150	13.552	11.400	1019.2	4.605
					160	13.974	12.289	1156.9	5.058
					170	14.330	13.147	1298.5	5.509
					180	14.630	13.975	1443.3	5.956
					190	14.887	14.773	1591.0	6.399
					200	15.11	15.54	1741.0	6.837
					210	15.30	16.28	1893.0	7.270
					220	15.47	17.00	2046.9	7.696
					230	15.61	17.69	2202.3	8.115
					240	15.74	18.36	2359.1	8.528
					250	15.86	19.00	2517.1	8.935
					260	15.96	19.63	2676.2	9.334
					270	16.05	20.23	2836.3	9.726
					280	16.13	20.82	2997.2	10.112
					290	16.20	21.38	3158.9	10.491
					298.15	16.26	21.83	3291.2	10.795
					300	16.27	21.93	3321.3	10.863
					325	16.39	23.24	3729.6	11.766
					350	16.48	24.46	4140.6	12.629

TABLE III. Electronic (Schottky) levels, ground-state manifold, for  $\gamma$ -type lanthanide sesquisulfides.

Compound, term, and $\Theta_{KW}$	Method of determination	Energy ( $\text{cm}^{-1}$ ) and level degeneracy ( $n$ )
$\text{Ce}_2\text{S}_3$ $\text{Ce}^{3+} ({}^2F_{5/2})$ $\Theta_{KW} = 63.65$	Opt. spectra/mag. suscept. Excess $C_p (K/W)$	0(2), 185(2), 358(2) 0(2), 185(2), 358(2)
$\text{Pr}_2\text{S}_3$ $\text{Pr}^{3+} ({}^3H_4)$ $\Theta_{KW} = 64.85$	Opt. spectra/mag. suscept. Lattice sum Excess $C_p (K/W)$	0(1), 12(1), 56(2), 165(1), 265(2), 280(1), 300(1) 0(1), 30(1), 100(2), 180(1), 270(2), 278(1), 282(1) 0(1), 15(1), 57(2), 165(1), 265(2), 280(1), 300(1)
$\text{Nd}_2\text{S}_3$ $\text{Nd}^{3+} ({}^4I_{9/2})$ $\Theta_{KW} = 66.03$	Optical spectra Excess $C_p (K/W)$	0(2), 76(2), 150(2), 180(2), 385(2) 0(2), 76(2), 150(2), 180(2), 385(2)
$\text{Pm}_2\text{S}_3$ $\text{Pm}^{3+} ({}^5I_4)$ $\Theta_{KW} = 67.20$	Lattice sum	0(1), 97(1), 140(1), 200(2), 237(2), 280(1), 346(1)
$\text{Sm}_2\text{S}_3$ $\text{Sm}^{3+} ({}^6H_{5/2})$ $\Theta_{KW} = 68.40$	Optical spectra Lattice sum Excess $C_p (K/W)$	0(2), 84(2), 194(2) 0(2), 84(2), 194(2), 1085(2), 1106(2), 1205(2), 1214(2) 0(2), 84(2), 194(2), 1188(2), 1196(2), 1211(2), 1214(2)
$\text{Eu}_2\text{S}_3$ $\text{Eu}^{3+} ({}^7F_0)$ $\Theta_{KW} = 69.60$	Lattice sum	0(1), 306(2), 337(1), 840(1), 892(1), 983(2), 1028(1)
$\text{Tb}_2\text{S}_3$ $\text{Tb}^{3+} ({}^7F_6)$ $\Theta_{KW} = 71.95$	Optical spectra/mag. suscept. Lattice sum Excess $C_p (K/W)$	0(1), 6(1), 29(1), 65(2), 130(2), 175(1), 190(1), 230(2), 300(1), 310(1) 0(1), 5(1), 24(1), 65(2), 130(2), 170(1), 185(1), 235(2), 298(1), 302(1) 0(1), 5(1), 27(1), 75(2), 130(2), 175(1), 190(1), 230(2), 330(1), 334(1)
$\text{Dy}_2\text{S}_3$ $\text{Dy}^{3+} ({}^6H_{15/2})$ $\Theta_{KW} = 73.10$	Optical spectra/mag. suscept. Lattice sum Excess $C_p (K/W)$	0(2), 52(2), 145(2), 190(2), 240(2), 265(2), 310(2), 550(2) 0(2), 43(2), 140(2), 190(2), 240(2), 280(2), 360(2), 600(2) 0(2), 59(2), 165(2), 200(2), 240(2), 265(2), 340(2), 590(2)

FIG. 2.  $\Theta_{KW}$ 's for  $\text{La}_2\text{S}_3$  and  $\text{Gd}_2\text{S}_3$ .

ence compounds are shown in Fig. 2. The excess contribution due to a magnetic transition in  $\text{Gd}_2\text{S}_3$  at low temperatures causes a local drop in apparent  $\Theta_{KW}$  for  $\text{Gd}_2\text{S}_3$  at these temperatures; apart from this— $\Theta_{KW}$  is constant over the entire temperature range.

For the evaluation of the lattice heat capacities of other  $\gamma$ -phase lanthanide sesquisulfides it was assumed that the input coefficients—and hence  $\Theta_{KW}$ —vary smoothly from one sample to the other. Figure 3 illustrates the trend of the LEM input coefficients, as well as that of the  $\Theta_{KW}$ 's, for each member of the subsystem. The sensitivity of the program to small variations in the coefficients and to the correspondence of molar volumes to atomic number is small enough to allow the use of a relationship linear in atomic number for interpolating these coefficients between related compounds without introducing a measurable error.

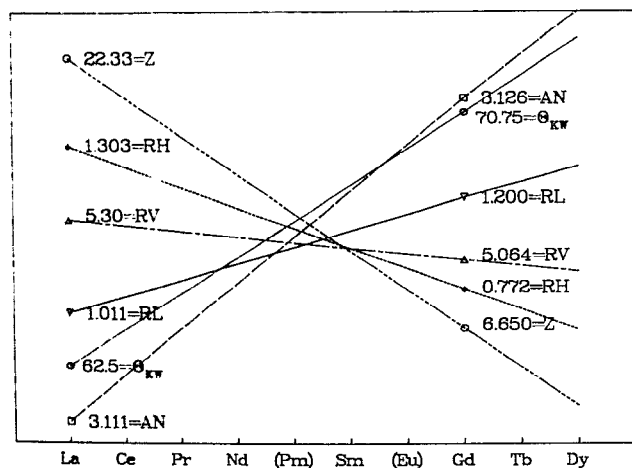


FIG. 3. Variation of the LEM input coefficients in the  $\gamma$ -phase  $\text{Ln}_2\text{S}_3$  subsystem. (The ordinate for each line is represented on a different scale.)  $\Theta_{KW}$  (the characteristic temperature) is an output from the LEM-1 program but an input in turn to LEM-2 and LEM-3. AN is the "effective" number of anions in a molecule, RL is an adjusting parameter, RV is the "effective" size of the primitive cell divided by the minimum interatomic spacing, RH is a mass related parameter, and Z is related to the number of molecules in a cell (adapted from Ref. 15).

Lattice heat capacities for all  $\gamma$ -phase lanthanide sesquisulfides were calculated by means of the LEM-3 computer program.<sup>15</sup> Figure 4 shows the lattice heat capacities for these compounds relative to that of  $\text{La}_2\text{S}_3$ . At low temperatures, mass effects dominate and the heat capacities of heavier cations tend to be larger. At intermediate temperatures, volume effects are dominant and thus the heat capacities of the lighter cations (with larger volumes—occasioned by the lanthanide contraction) are larger. Nearer ambient temperatures, all compounds tend towards the Dulong–Petit limit.

Figure 5 shows the calorimetric and spectroscopic Schottky contributions for  $\text{Ce}_2\text{S}_3$  through  $\text{Dy}_2\text{S}_3$ . The experimental calorimetric (mainly Schottky) excess heat-ca-

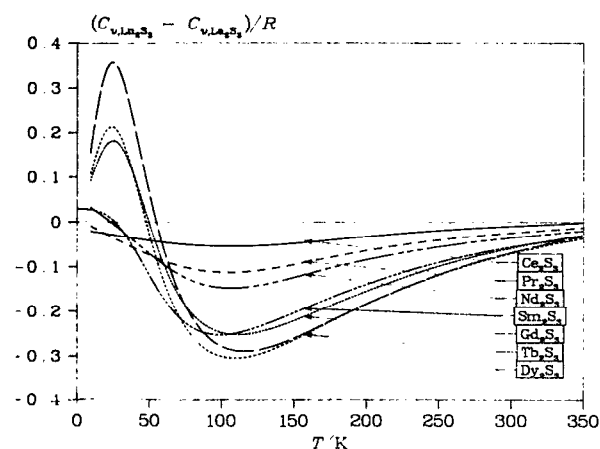


FIG. 4. Lattice heat capacities for the  $\gamma$ -phase lanthanide sesquisulfides relative to that of  $\text{La}_2\text{S}_3$ .

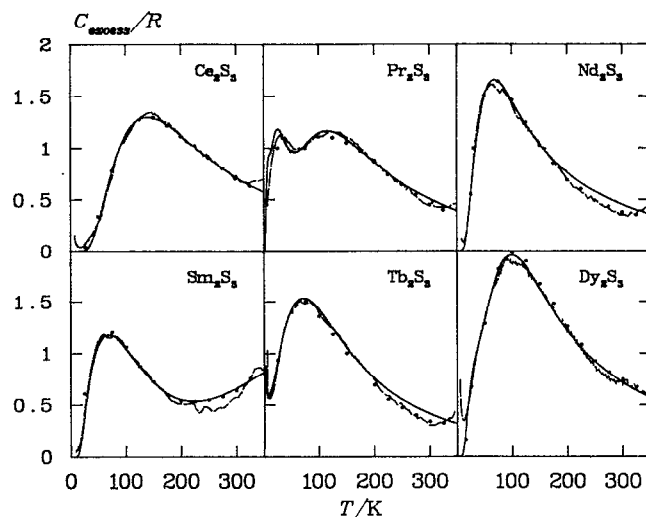


FIG. 5. Excess heat capacities for the  $\gamma$ -phase lanthanide sesquisulfides. Dashed lines—calorimetric (Komada/Westrum); solid lines—spectroscopic; the points are representative values from the volumetric priority approach (Refs. 1 and 2). (The dashed lines are based on the experimental values which reflect the small magnitude of the experimental uncertainty.)

capacity contribution—by the Komada/Westrum method, and by the volumetric priority approach, and the Schottky contribution calculated from the spectral data are compared. The energy levels that were selected for matching the excess heat capacity and the identified spectroscopic values and their degeneracies are listed in Table III. Good agreement was obtained between the fitted heat capacities and the experimental excess values for all compounds. The concave upward trend of the excess contribution at superambient temperatures for  $\text{Sm}_2\text{S}_3$  may imply the onset of thermal excitation of the electrons to higher energy levels. The Komada/Westrum values for the lattice heat capacities seem to

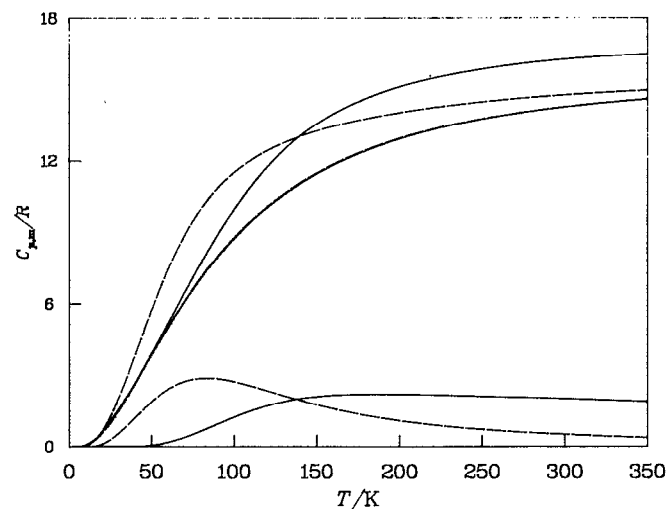


FIG. 6. In sequence of increasing magnitude: calculated Schottky, lattice, and total heat capacities for  $\text{Eu}_2\text{S}_3$ —solid lines, and  $\text{Pm}_2\text{S}_3$ —dashed lines.

be comparable to results that were found for these compounds by means of the volumetric priority approach.<sup>1,2</sup> The fact that the simplified, essentially empirical, volumetric priority lattice heat capacities are in such good agreement with those of the phonon distribution method (essentially a single parameter, enhanced Debye approach) provides reassurance of the reliability of both, under these constraints of application—as has already been argued elsewhere.<sup>31</sup> Further substantiation and rationalization for the dependence of entropy and heat capacity upon volume has been provided for another chemical system by Holland.<sup>32</sup>

### Thermodynamic values for europium and promethium sesquisulfides

$\text{Eu}_2\text{S}_3$  and  $\text{Pm}_2\text{S}_3$  were not studied experimentally in this research; the synthesis of  $\text{Eu}_2\text{S}_3$  was unsuccessful because  $\text{Eu(II)}$  is chemically more stable than  $\text{Eu(III)}$  in the sulfide lattice, and the most stable promethium isotope,  $^{145}\text{Pm}$ , is radioactive with a half-life of 18 years.

The lattice heat capacities of  $\text{Eu}_2\text{S}_3$  and  $\text{Pm}_2\text{S}_3$  interpolated from those of  $\text{La}_2\text{S}_3$  and  $\text{Gd}_2\text{S}_3$  by using the LEM-2 program, with input coefficients interpolated from Fig. 3, are included in Fig. 6. The Schottky contributions for  $\text{Eu}_2\text{S}_3$  and  $\text{Pm}_2\text{S}_3$  were evaluated using the lattice-sum approach to obtain the crystal-field splitting of the  $^{2S+1}L_J$  multiplets.<sup>2</sup> As in other  $\gamma$ -phase sesquisulfides, the cations in  $\text{Eu}_2\text{S}_3$  and  $\text{Pm}_2\text{S}_3$  have  $S_4$  symmetry. For  $\text{Eu}_2\text{S}_3$ , the ground state level is  $^7F_0$ . A set of two electronic levels (one doubly degenerate and one singly degenerate), associated with the  $^7F_1$  manifold, is predicted at about  $300\text{ cm}^{-1}$  above the ground state, and a second set, consisting of one doubly degenerate and three nondegenerate levels, associated with the  $^7F_2$  manifold, is predicted between  $800$  and  $1000\text{ cm}^{-1}$  above the ground state. The crystal-field splitting of the  $^7F_1$  and  $^7F_2$  manifolds contribute to the calculated subambient Schottky heat capacity of  $\text{Eu}_2\text{S}_3$ . The ground-state manifold of  $\text{Pm}_2\text{S}_3$ ,  $^5I_4$ , was calculated on the basis of the crystal-field splitting obtained using parameters deduced from a lattice-sum calculation. The selected energy levels for  $\text{Eu}_2\text{S}_3$  and  $\text{Pm}_2\text{S}_3$  are presented in Table III. The calculated lattice, Schottky, and total heat capacities for these two compounds are presented in Fig. 6. Thermodynamic functions at selected temperatures are presented in Table II. No magnetic contributions are attributed to the heat capacity of either compound.

### ACKNOWLEDGMENT

A portion of the evaluation, performed at the University of Illinois at Chicago was supported by the Solid State Chemistry program of the National Science Foundation, through Grant No. DMR-8815798.

- <sup>1</sup> E. F. Westrum, Jr., R. Burriel, J. B. Gruber, P. E. Palmer, B. J. Beaudry, and W. A. Plautz, *J. Chem. Phys.* **91**, 4838 (1989).
- <sup>2</sup> J. B. Gruber, R. Burriel, E. F. Westrum, Jr., P. E. Palmer, B. J. Beaudry, and W. A. Plautz, *J. Chem. Phys.* **95**, 1964 (1991).
- <sup>3</sup> J. R. Henderson, M. Muramoto, E. Loh, and D. M. Johnson, *Purification and Growth of Rare-Earth Compound Semiconductors 1966*, DAC-59368 P (McDonnell-Douglas Astronautics, Santa Monica).
- <sup>4</sup> J. R. Henderson, M. Muramoto, E. Loh, and J. B. Gruber, *J. Chem. Phys.* **47**, 3347 (1967).
- <sup>5</sup> J. B. Gruber, J. R. Henderson, M. Muramoto, and E. Loh, *Bull. Am. Phys. Soc. II* **14**, 310 (1969).
- <sup>6</sup> J. R. Henderson, M. Muramoto, J. B. Gruber, and R. Menzel, *J. Chem. Phys.* **52**, 2311 (1970).
- <sup>7</sup> E. F. Westrum, Jr., *Pure Appl. Chem.* **55**, 539 (1983).
- <sup>8</sup> J. B. Gruber, R. D. Chirico, and E. F. Westrum, Jr., *J. Chem. Phys.* **76**, 4600 (1982).
- <sup>9</sup> E. F. Westrum, Jr., *J. Chem. Thermodyn.* **15**, 305 (1983).
- <sup>10</sup> R. D. Chirico, E. F. Westrum, Jr., J. B. Gruber, and J. Warmkessel, *J. Chem. Thermodyn.* **11**, 835 (1979).
- <sup>11</sup> R. D. Chirico and E. F. Westrum, Jr., *J. Chem. Thermodyn.* **12**, 71 (1980).
- <sup>12</sup> R. D. Chirico, E. F. Westrum, Jr., and J. B. Gruber, *J. Chem. Thermodyn.* **12**, 311 (1980).
- <sup>13</sup> R. D. Chirico and E. F. Westrum, Jr., *J. Chem. Thermodyn.* **13**, 519 (1981).
- <sup>14</sup> R. D. Chirico and E. F. Westrum, Jr., *J. Chem. Thermodyn.* **13**, 1087 (1981).
- <sup>15</sup> N. Komada, Dissertation, University of Michigan, Ann Arbor, 1985.
- <sup>16</sup> E. F. Westrum, Jr. and N. Komada (manuscript in preparation).
- <sup>17</sup> N. Komada, *Netsu Sokuti* **17**, 25 (1990).
- <sup>18</sup> E. F. Westrum, Jr. and N. Komada, *Thermochim. Acta.* **109**, 11 (1988).
- <sup>19</sup> B. J. Beaudry and K. A. Gschneidner, Jr., *Handbook on the Physics and Chemistry of Rare Earths*, edited by K. A. Gschneidner, Jr. and L. Eyring (North-Holland, Amsterdam, 1978), Vol. 1, p. 173.
- <sup>20</sup> American Smelting and Refining Company, Denver, Colorado.
- <sup>21</sup> M. Picon, L. Domange, J. Flahaut, M. Guittard, and M. Patrie, *Bull. Soc. Chim. Fr.* **1960**, 221.
- <sup>22</sup> E. D. West and E. F. Westrum, Jr., in *Experimental Thermodynamics*, edited by J. P. McCullough and D. W. Scott (Butterworths, London, 1968), Vol. 1, p. 333.
- <sup>23</sup> E. F. Westrum, Jr., in *Thermochemistry and its Applications to Chemical and Biochemical Systems*, edited by M. A. V. Ribeiro da Silva (Reidel, Dordrecht, Holland, 1984), p. 754.
- <sup>24</sup> J. R. Henderson, D. M. Johnson, and M. Muramoto, Production of High Purity Rare Earth Sulfides, U.S. Patent No. 3748095, Issued July 24, (1973), owned by McDonnell-Douglas Corp., Long Beach, CA 90846.
- <sup>25</sup> J. R. Henderson, M. Muramoto, D. M. Johnson, and E. Loh, *Purification and Growth of Rare Earth Sesquisulfide Semiconductor Crystals*, Douglas Paper 4415, Douglas Aircraft Company, Santa Monica, CA. IRAD Program 88001-700 (1967).
- <sup>26</sup> J. B. Gruber, Department of Physics, Portland State University, 1984 (unpublished).
- <sup>27</sup> J. Flahaut, *Handbook on the Physics and Chemistry of Rare Earths*, edited by K. A. Gschneidner, Jr. and L. Eyring (North Holland, Amsterdam, 1979), Chap. 31, p. 1.
- <sup>28</sup> J. B. Gruber, R. P. Leavitt, and C. A. Morrison, *J. Chem. Phys.* **79**, 1664 (1983).
- <sup>29</sup> J. B. Gruber, *Bull. Am. Phys. Soc.* **32**, 1053 (1987).
- <sup>30</sup> See for example: R. Shaviv, *Dissertation*, University of Michigan, Ann Arbor (1988); R. Shaviv, E. F. Westrum, Jr., F. Gronvold, S. Stølen, A. Inaba, H. Fujii, and H. Chihara, *J. Chem. Thermodyn.* **21**, 631 (1989); R. Shaviv, E. F. Westrum, Jr., R. J. C. Brown, M. Sayer, X. Yu, and R. D. Weir, *J. Chem. Phys.* **92**, 6794 (1990).
- <sup>31</sup> E. F. Westrum, Jr., *Can. J. Chem.* (in press, 1991).
- <sup>32</sup> T. J. B. Holland, *Am. Mineral* **74**, 5 (1989).